Food Packaging and Shelf Life 39 (2023) 101140

Contents lists available at ScienceDirect

Food Packaging and Shelf Life

journal homepage: www.elsevier.com/locate/fpsl

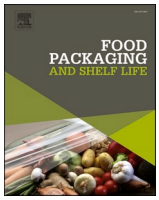

Performance of bacterial nanocellulose packaging film functionalised *in situ* with zinc oxide: Migration onto chicken skin and antimicrobial activity

Francisco A.G. Soares Silva [a,b,c], Teresa Bento de Carvalho [a], Fernando Dourado [b,c], Miguel Gama [b,c], Paula Teixeira [a], Fátima Poças [a,d,*]

[a] Universidade Católica Portuguesa, CBQF-Centro de Biotecnologia e Química Fina – Laboratório Associado, Escola Superior de Biotecnologia, Rua Diogo Botelho 1327, 4169-005 Porto, Portugal
[b] Centre of Biological Engineering, University of Minho, Campus de Gualtar, 4710-057 Braga, Portugal
[c] LABBELS—Associate Laboratory, 4710-057 Braga, Portugal
[d] Universidade Católica Portuguesa, Center for Quality and Food Safety (CINATE), Escola Superior de Biotecnologia, Portugal

ARTICLE INFO

Keywords:
Bacterial nanocellulose
Zinc oxide
Nanoparticles
Active packaging
Migration

ABSTRACT

Zinc oxide nanoparticles (ZnO) are cost-effective antimicrobial agents with great potential for the active packaging industry. Bacterial NanoCellulose (BNC) features a porous fibre network, with high absorption capacity, flexible and with good mechanical properties, suitable as a carrier of active agents. In this work, BNC_{ZnO} films were developed and optimized regarding the particle size and ZnO concentration. The NaOH dropwise addition to BNC membranes immersed in $Zn(CH_3COO)_2$-PVOH enabled the production of ZnO nanoparticles with an z-average of 144 nm and a low polydispersity index. High ZnO incorporation (~27%m_{Zn}/m_{BNCZnO}) was obtained, with uniform distribution all over the BNC membranes. These composites were then characterized and evaluated for Zn migration using food simulants (10%, 20%, and 50% ethanol) with results lower than the limit. Migration into chicken skin, as a real food model, was low at 4 °C but exceeded the migration limit at 10 and 22 °C. Zn migration was also found to be temperature and pH dependent. When applied to chicken skin, BNC_{ZnO} was effective against *E. coli*, *Salmonella* (0.5–1.0 log reduction), and *Campylobacter* spp. (2.0 log reduction), indicating its potential for active packaging applications.

1. Introduction

Active and intelligent packaging has gained significant attention from both industry and research communities, as evidenced by the growing number of publications in the field (Vilela et al., 2018). Active packaging may be characterized by its ability to absorb or release substances to extend food shelf life, preserve freshness and enhance safety (by inhibiting pathogenic bacteria). In turn, intelligent packaging monitors the condition of the packaged food (and the surrounding environment), offering valuable information for effective food preservation (Gregor-Svetec, 2018). Both systems have been explored using bio-based polymers such nanocellulose, chitosan, polylactic acid and polyhydroxyalkanoates as alternatives to petroleum-based plastics (Cerqueira et al., 2018; Kishore et al., 2023). It has been reported that nanocomposite systems often improve the mechanical and barrier properties of neat biobased polymers, which is crucial for producing packaging systems that meet the food protection requirements (Silva, et al., 2020). However, the high manufacturing costs, difficult scalability and low global production of these bio-based composites still make them uncompetitive when compared to petroleum-based plastics (Ibrahim et al., 2021; Silva et al., 2020). The functionalization of composites with active agents, through low-cost strategies, may be a step toward increasing their competitiveness.

One of the major bio-based polymers being studied is nanocellulose, which is known for its high crystallinity, degree of polymerization and mechanical strength, low density, biocompatibility, non-toxicity and biodegradability. Nanocellulose is an excellent support or carrier for active substances, such as bacteriocins, metal oxides and organic acids (Silva et al., 2020). Nanocellulose may be isolated from plants or produced through bacterial fermentation (Jedrzejczak-Krzepkowska et al., 2016; Silva et al., 2020). Plant-based nanocellulose extraction requires chemicals and intensive wood processing (steam explosion,

* Corresponding author at: Universidade Católica Portuguesa, CBQF-Centro de Biotecnologia e Química Fina – Laboratório Associado, Escola Superior de Biotecnologia, Rua Diogo Botelho 1327, 4169-005 Porto, Portugal.
E-mail address: fpocas@ucp.pt (F. Poças).

https://doi.org/10.1016/j.fpsl.2023.101140
Received 28 March 2023; Received in revised form 19 July 2023; Accepted 20 July 2023
Available online 31 July 2023

enzyme-assisted and acid hydrolysis and/or other mechanical methods), which are not free of environmental issues (de Amorim et al., 2020). As an alternative, bacterial nanocellulose (BNC) may be used. BNC is a biopolymer produced by bacteria (*Komagataeibacter genus)*, using either static or agitated fermentation, and thus through a more sustainable approach (Jedrzejczak-Krzepkowska et al., 2016). When compared to plant nanocelluloses, BNC is naturally produced by static culture as a membrane with high porosity and water holding capacity, mechanically stable in the wet state (Wang et al., 2019). For food packaging applications, BNC has been studied either as a reinforcing agent (Dileswar et al., 2022), as the main matrix (Almasi et al., 2019; Pan et al., 2023) as well as a carrier for active agents (Cazón & Vázquez, 2021; Vilela et al., 2019).

Zinc oxide (ZnO) is a thermally stable material with photocatalytic and antibacterial activity. In addition, ZnO is well known for its low production cost and for being easily scalable and processable. It is widely used in applications such as drug delivery, cosmetics and medical devices (Wojnarowicz et al., 2020). So far, it is considered safe for food contact materials (FCMs) by the European Food Safety Authority (EFSA), as an ultraviolet light absorber in unplasticized polymers at up to 2.0% (m/m) (EFSA CEF Panel, 2017). More recently, ZnO has been explored in its nano form, since its higher surface area may result in enhanced properties, especially antimicrobial activity (Kim et al., 2022). The research community has focused on the relationship between nanoparticle (NP) size and its antimicrobial effect (Kumar et al., 2017; Sirelkhatim et al., 2015). However, only few studies have focused on ZnO migration into food systems (Hakeem et al., 2020; Olaimat et al., 2022; Polat et al., 2018).

In Regulation (EC) No 1935/2004 it is outlined that food contact materials (FCMs) must be designed (according to good practices) to prevent migration of their constituents, such that the transferred quantities do not pose a risk to human health, undesirable changes in the food composition, or deterioration of its organoleptic properties. Furthermore, the regulations relating to plastic materials, namely Regulation (EU) No. 10/2011, and active and intelligent packaging materials (Regulation (EC) No. 450/2009), highlight the need for a specific evaluation of substances in nanoform. Thus, it is imperative to understand the potential for mass transfer of nanoparticles (NPs) and the interactions between the composite materials and the food systems (Poças & Franz, 2018).

In a scientific study regarding the safety assessment of ZnO nanoparticles in FCMs, EFSA concluded that ZnO NPs do not migrate in nanoform, when incorporated in an unplasticized polymer (Commission, 2007; EFSA CEF Panel, 2017). Consequently, the safety assessment should focus on the migration of soluble ionic zinc (Zn^{2+}), which must comply with the specific migration limit (SML) of 5 mg kg^{-1} (Commission, 2007; EFSA CEF Panel, 2017). The migration of ZnO depends on the matrix where it is incorporated, with several polymers having been tested, such chitosan, gelatin, starch and nanocellulose (Silva et al., 2020).

The longer fibres, superior water holding capacity and porosity of BNC are considered to be appropriate for active food packaging, since it makes relatively easy to incorporate active substances (Jedrzejczak-Krzepkowska et al., 2016; Vilela et al., 2019). The literature reports the use of BNC as a support for many active agents (Choo et al., 2021; Missio et al., 2018; Tsai et al., 2018; Zhang, et al., 2017), and for ZnO in particular (Pirsa et al., 2018; Wahid et al., 2019). These studies described the optimization of the *in situ* production or incorporation of ZnO on BNC, considering its concentration, morphology and particle size, to obtain the most effective antimicrobial activity. While reported research has predominantly focused on the antimicrobial efficiency of ZnO functionalized nanocellulose films, studies concerning the migration of Zn (from ZnO) have received limited attention, particularly migration to food models. Hence, in this study, the Zn migration from BNC_{ZnO} films is addressed, along with its antimicrobial activity using a real food model, chicken skin.

The production of ZnO in a wet thin BNC membrane was studied, using two different *in situ* production methods. Most of the published work used *in situ* production of ZnO through direct immersion of the BNC membrane. In the present work an alternative *in situ* drop-wise production method was tested. ZnO morphology, particle size, particle distribution within the BNC membrane and ZnO concentration were optimized to obtain the best performing composite for active food packaging. The dried composite was then tested for migration using food simulants as well as a real food model, chicken skin. These tests were conducted at different temperatures, and the Weibull model was used to describe the Zn migration from BNC. Finally, the antimicrobial activity of BNC films with ZnO was tested using the same real food model. This model was selected because BNC_{ZnO} is envisaged as an antimicrobial packaging film for fresh/conditioned chicken.

2. Materials and methods

2.1. BNC production and purification

The strain *Komagataeibacter xylinus* ATCC 700178 (American Type Culture Collection) was cultured in solid state using Hestrin-Schramm (HS) medium supplemented with 2.0% (w/v) agar (Acros Organics, Geel, Belgium). For pre-inoculum, 100 mL of Hestrin-Schramm culture medium (HS) was prepared in a 1 L conical flasks (Hestrin & Schramm, 1954). HS culture is composed of the following components (in % m/v): 2.0 glucose (Fluka, Buchs, Switzerland), 0.5 peptone (Himedia, Pennsylvania, USA), 0.5 yeast extract (Fisher, Massachusetts, USA), 0.339 disodium phosphate di-hydrated (Panreac, Barcelona, Spain) and 0.126 citric acid (Panreac). HS medium was autoclaved at 121 °C for 20 min. The cells from the HS-agar were inoculated onto the previously prepared HS medium using an inoculation loop and incubated under static conditions for 48 h. The resulting cellulose formed was manually agitated to release the bacteria trapped within the cellulose matrix into the medium. This medium was subsequently used for further inoculations at a 10% (v/v) ratio to the final fermentation volume of fresh HS medium. The inoculated fresh culture medium was incubated in cuvettes (10×20×10 cm) at 30 °C for 15 days (at a fixed culture medium depth of 1.5 cm). After 15 days of static fermentation, produced BNC membranes were washed with 0.1 M NaOH (Panreac) at room temperature to remove any residual culture medium and trapped cells. Subsequently, the membranes were washed with distilled water at room temperature, with multiple water changes, until neutral pH. The membranes were then stored in distilled water at 4 °C until further use.

2.2. ZnO NPs and BNC_{ZnO} production

The BNC membranes were longitudinally sliced into thinner membranes with a thickness of 2.0 mm using a Duegi Affettatrici machine (type 275-SE, Besnate, Italy). Subsequently, disks with diameters of 9.0 mm, 13.0 mm, and 20.0 mm were prepared from these BNC membranes. The 13.0 mm disks were used for optimizing the production of BNC_{ZnO}, while the 9.0 mm disks were employed to assess Zn migration in food simulants. The 20.0 mm disks, were used for Zn migration and antimicrobial testing in chicken skin. The BNC disks were frozen in liquid nitrogen and subsequently lyophilised in a freeze drier (Coolsafe 100–9 Pro, Labogene, Allerød, Denmark) at − 99 °C and 0.025 mbar until complete dryness.

Prior to ZnO *in situ* production, two approaches were studied without BNC disks: (i) *in situ* and (ii) drop *in situ*. The *in situ* method (i), consisted of the direct addition of 10 mL of NaOH (0.05 M) solution into 2.0 mL solution of $Zn(CH_3COO)_2 0.2\ H_2O$ (0.01 M) (Sigma; India), at room temperature, to obtain a ZnO suspension. For the drop *in situ* method (ii), the ZnO NPs synthesis was carried out as follows: a 20 mL NaOH solution (1 M) was added dropwise (0.67 $mL.min^{-1}$; using a syringe pump (New Era Pump systems, Farmingdale, NY) to 100 mL solution of Zn $(CH_3COO)_2$ (0.01–0.1 M), with magnetic stirring at 200 rpm and at

50 °C. After 1 h, the ZnO suspension was collected for washing. These ZnO NPs were produced, using glycerol (Fisher, Belgium;0.5%m/v) and polyvinyl alcohol (PVOH; FLuka, Germany) (0.5%m/v) as capping agents for ZnO NPs optimization (Sirelkhatim et al., 2015). The obtained ZnO suspension was then washed with ultra-pure water by centrifugation (Eppendorf Centrifuge 5430 R; Germany) at 4000 rpm until neutral pH. Then, ZnO NPs were stored in the fridge for 1 day, before dynamic scattering analysis.

For ZnO *in situ* production (on BNC disks), only the drop *in situ* was carried out as *in situ* method had a lower performance regarding particle size and polydispersity (Section 3.1. Characterization of the ZnO particles and films). The *in situ* ZnO synthesis was carried out as follows: a 20 mL NaOH solution (1 M) was added dropwise (0.67 mL.min^{-1}; using a syringe pump (New Era Pump systems) to 100 mL solution of Zn $(CH_3COO)_2$ (0.01–0.05 M) with previously immersed (swollen) BNC disks (magnetic stirring at 200 rpm and 50 °C was applied). The BNC disks were left overnight under stirring and then washed with ultra-pure water until neutral pH, before air drying at 37 °C (in a hot room). All disks (9.0 mm and 13.0 mm diameter disks with an average thickness of 20 μm and 20.0 mm diameter disks with an average thickness of 40 μm) were stored in a desiccator until use. The water holding capacity of BNC disks, determined by the ratio of the mass of removed water (g) to the mass of dried BNC (g), was found to be 85.3 ± 13.8 (g of water removed/g of dried cellulose).

2.3. Physical characterization

BNC thickness - measurements were performed with a digital thickness gauge (Adamel Lhomargy, France) on all produced BNC disks. Three replicates were prepared for each sample and five thickness measurements (at random positions) were taken for each replicate.

Dynamic scattering analysis (DLS) - The size of the ZnO NPs was estimated using a Zetasizer NanoZS (Malvern Instruments Ltd., Worcestershire, UK). Five measurements were taken from each suspension to obtain an average size (nm) and average polydispersity (PdI). Before analysis, ZnO NPs suspensions were subjected to ultrasonication (UW 2070, Bandelin Sonoplus) with 40% amplitude for 4 min

Morphologic analysis - Neat BNC and BNC_{ZnO} samples were characterised using a desktop Scanning Electron Microscope (SEM) coupled with energy-dispersive spectroscopy (EDS) analysis (Quanta 650). Prior testing, all samples were frozen in liquid nitrogen, sliced perpendicularly and subsequently lyophilised as previously described. All results were processed with ProSuite software. The samples were placed in an aluminium pin stub with electrically conductive carbon adhesive tape (PELCO Tabs™). Samples were coated with 1 nm of Au (10 Angstrom) for improved conductivity. The analysis was conducted with intensity image of 10 kV, reduced vacuum and a varying magnification scale from x1000 to x5000. The size of ZnO NPs was measured through ImageJ software (version 1.8.0).

Fourier-Transform Infrared Spectroscopy (FTIR)- FTIR analysis of BNC, BNC_{ZnO} and ZnO (dry-state) was carried out in a Bruker FTIR spectrometer ALPHA II (Bruker Corporation, Billerica, MA, USA) in transmission mode, operating at a resolution of 4 cm^{-1}. The spectra were taken between 4000 and 300 cm^{-1} by averaging 60 scans for each spectrum. All samples were scanned twice for verification purposes.

2.4. Migration tests into food simulants and into chicken skin

2.4.1. Food simulants

The specific migration of zinc from BNC_{ZnO} films (0.05 M ZnO) into food simulants (ethanol 10%, 20% and 50% (v/v)) as well as into chicken skin was determined. For the food simulants tests, a solid-to-liquid ratio of 2.7 dm^2 L^{-1} was used. The BNC_{ZnO} disks were immersed in the food simulant at 60 °C for more than 10 days, following Regulation (EU) No. 10/2011 applicable to plastics. During the assay, samples were collected after 1, 3, 5, 7 and 15 days. The simulant samples were analysed for Zn concentration (Section 2.5).

2.4.2. Chicken skin

The skin from a chicken leg, purchased at a local supermarket, was carefully removed in one piece and stored refrigerated until use. The skin was kept for a maximum of 3 days. The water content of the skin was about 42% (m/m). The skin was cut into disks of similar size to the BNC_{ZnO} disk (20 mm). BNC_{ZnO} disks (average weight of 15 mg) were brought into contact with the chicken skin disks, resulting in a solid-to-solid ratio of 44.3 dm^2 kg^{-1}. The BNC_{ZnO} disk and the skin were left in contact for 7 days at 4 °C, 10 °C and 22 °C. This temperature range was chosen to simulate the different temperature conditions that the food may be exposed to, the first being the recommended one for storage and the two other representing abuse temperatures. Chicken skin samples were collected after 1, 3, 5 and 7 days for determination of Zn concentration. The chicken skin disks were digested as described in Section 2.5 before zinc determination.

The Zn concentrations obtained (either on food simulants or chicken skin) were normalized to the conventional contact ratio of 6 dm^2 kg^{-1}.

2.5. Zinc quantification

The concentration of Zn in BNC, BNC_{ZnO}, in food simulants and chicken skin was quantified by Atomic Absorption Spectrophotometer (AAS) according to standard EN 14084. The concentration of Zn in the food simulants was determined directly and after microwave digestion in the case of BNC_{ZnO} samples and chicken skin, as described below. As control, the amount of Zn on BNC and chicken skin was determined and found to be 0.012% m/m_{BNC} and 0.0008% m/$m_{chicken}$, respectively.

Samples preparation by microwave digestion - samples were prepared following the guidelines of standard EN 13804 (European Standard, 2013): BNC_{ZnO} disks (*ca* 15 mg) and chicken skin (*ca* 0.2 g) were separately ground into small pieces and evenly weighed into the digestion vessel; then, 5 mL nitric acid 65% (HNO_3) (Panreac, Spain) and 2 mL of hydrogen peroxide (H_2O_2) (Merck KGaA, Germany) were added; finally, the samples were submitted to the microwave digestion program (Speedwave MWS-3 +, Berghof, Germany), presented in supplementary material (Table S1). After microwave treatment, the digested samples were diluted with ultra-pure water to a final volume of 50 mL and analysed by AAS.

Atomic absorption spectroscopy - an atomic absorption spectrophotometer (Perkin Elmer Aanalyst 400, Waltham, MA) was used, equipped with a zinc cathode lamp ($\lambda = 213.9$ nm). Whenever necessary, samples were diluted with ultra-pure water to obtain an absorbance signal within the Zn concentration (0–0.50 mg L^{-1} of Zn). Working solutions of zinc (0–0.50 mg L^{-1} of Zn) were previously prepared using a stock solution of 1000 mg L^{-1}, using a 1.0% v/v HNO_3 solution. Five readings were made for all samples and working solutions. The system suitability parameters were determined: limit of detection (LoD – 0.07 mg L^{-1}) and limit of quantification (LoQ - 0.14 mg L^{-1}). All samples had concentrations higher than LoD or LoQ. For the determination of zinc in the migration solutions, working solutions (0–0.50 mg L^{-1} of Zn) were prepared with the food simulants used for the migration tests (ethanol 10%, 20% and 50% v/v) (Honeywell, Germany).

2.6. Migration modelling

A kinetic model based on the Weibull distribution function (Hallinan, 1993) was used to describe Zn migration from BNC into chicken skin. The Weibull model was previously applied to describe migration of different substances from plastics and from paper onto simulants (Poças et al., 2011; Poças et al., 2012). This model is empirical and mathematically simpler than the models describing diffusion according to Fick's law (Poças et al., 2012) and is represented by the Eq. (1):

$$C(t) = C\infty * \left(1 - \exp\left(-\left(\frac{t}{\tau}\right)^{\beta}\right)\right) \quad (1)$$

Where *C(t)* is the concentration of migrant in food simulant changing with time (t) and C∞ is the concentration at equilibrium. The model has two parameters: τ, the system time constant, which represents the process rate, and β, the shape parameter, which relates to the initial rate of the process, quantifying the pattern of the curvature observed (Poças et al., 2012). This model was fitted to the experimental data obtained in the migration tests for each temperature and the parameters C∞ , β and τ were estimated as described in Section 2.8.

The effect of temperature on the parameters τ and β was analysed considering the Arrhenius equation (Fig. 5), with the general formula:

$$K = A\exp(-\frac{Ea}{RT}) \quad (2)$$

Eq. (2) after natural log becomes

$$\ln(K) = \ln(A) - \frac{Ea}{R}\frac{1}{T} \quad (3)$$

which can be written using the form y = ax + b; where "y" represents "ln(τ)" or "ln(β)"; "x" represents "$1/T$"; and "a" and "b" constants stands for " $-Ea/R$" and "ln(A)", respectively.

2.7. Antimicrobial activity of BNC_{ZnO} disks

The antimicrobial activity of the BNC_{ZnO} disks on chicken skin was explored by the viable cell counting method. Cocktails of different *Salmonella* serotypes and different strains of *C. coli* and *C. jejuni* were prepared for testing. The composition of the cocktails is shown in supplemental material (Table S2), together with the source of each bacteria strain. All tests were performed in duplicate and validated twice.

2.7.1. Inocula preparation and viable cell count on chicken skin

E. coli ATCC 25922 *and Salmonella* (*S.* Enteritidis 545047 and cocktail strains*)* were grown on Tryptic soy Agar (TSA) (BIOKAR, France) at 30 °C for 24 h. For *Campylobacter* (*C. coli* DSM4689 and cocktail strains), cultures were grown in modified charcoal cefoperazone deoxycholate agar (MCCD agar; SARSTEDT) at 42 °C, in microaerophilic conditions (5.6% CO_2) for 48 h. Then, colonies were transferred to Ringer's solution (BIOKAR) to obtain an optical density (OD_{600}) of 1.0, equivalent to 10^9 CFU mL^{-1}. Cocktails (from *Salmonella* and *Campylobacter*) were prepared by mixing equal volumes of each strain from the same genus, in Ringer's solution.

Afterwards, 10 μL (10^9 CFU mL^{-1}) of each culture or cocktail were inoculated on chicken skin samples, of the same diameter as that of BNC/BNC_{ZnO} disks. The contaminated chicken skin samples were stored for 24 h at 4 °C, to verify that bacteria counts were maintained before applying the BNC disks. Then, BNC and BNC_{ZnO} disks were placed on top of the contaminated samples and stored again for 24 h (48 h since inoculation) at 4 °C. Contaminated chicken skin samples (at 0 h′, 24 and 48 h) were submerged into Ringer's solution (9 mL) and manually diluted (1:10 mL) until 10^5 CFU mL^{-1}. Further dilutions (until 10^1 CFU mL^{-1}) were automatically made with spiral plate (easySpiral-Pro, Interscience). After inoculation, cells on each contaminated sample were counted after 15 min (referred as 0 h′), 24 h and 48 h. In parallel, the number of active growing cells on contaminated chicken skin (without BNC/BNC_{ZnO} treatment) was monitored throughout the assay. The cell reduction was quantified as follows:

$$Reduction = Log\left(\frac{n}{n0}\right) \quad (4)$$

Where "n" corresponds to the CFU mL^{-1} after exposure of the chicken skin to BNC/BNC_{ZnO} for a certain time (from 24 h to 48 h after inoculation) and "n0″ corresponds the initial concentration (CFU.mL^{-1}), before exposure. Chicken skin inoculated and without any BNC disk was also stored for reference. Viable cell counting was also done on uncontaminated chicken skin samples, where no bacteria growth was observed.

2.8. Data handling and statistical analysis

Statistical analysis was supported by Prism version 9.4.1 (GraphPad Software, La Jolla California USA), using one-way (and two-way) ANOVA and Tuckey's post-hoc analysis for pairwise comparison of more than two means. Mean differences were considered statistically non-significant (ns) when p-value was higher than 0.05 (95% of interval of confidence). The default statistical confidence level was considered to be 95% ($P < 0.05$) in all tests. Weibull model parameters were estimated with SPSS Statistics software (IBM, Armonk, NY) version 27 by non-linear estimation, using the Levenberg-Marquardt algorithm to minimise the sum of the squares of the differences between the predicted and experimental values. The regression quality was assessed by residuals analysis (normality and randomness), the confidence intervals and the coefficient of correlation R^2.

3. Results and discussion

3.1. Characterization of the ZnO particles and films

3.1.1. Size and polydispersity of ZnO particles synthetised in different conditions

It is well known that the antimicrobial efficiency of ZnO highly depends on particle size, morphology and dosage (Sirelkhatim et al., 2015). Lowering the particle size, thus increasing the specific surface area, improves the reactivity of ZnO against bacteria. In this work, *in situ* and drop *in situ* methods were optimized in what concerns ZnO particle size and its polydispersity, attempting to obtain small particles. The two methods were compared and the use of capping agents (PVOH and glycerol) were used to lower the particle size by preventing ZnO aggregation. Capping agents were compared regarding the performance of producing ZnO with low particle size and without agglomeration. This optimisation was performed in experiments without BNC.

As can be seen in Fig. 1, the methodology Drop *in situ* provided lower ZnO particles sizes (144–211 nm) than the *in situ* approach (278–455 nm). When PVOH was used as the capping agent, the particle size slightly decreased from 208 to 144 nm (Fig. 1.a). Despite not being statistically different, a downtrend polydispersity index is observed when PVOH was used, providing therefore more homogeneous ZnO suspensions (Fig. 1b)). As compared to the control, when glycerol was used as capping agent, particle size increased when using *in situ*. Glycerol had no major effect when using Drop *in situ* (Fig. 1.a). Hence, the Drop *In situ* method and PVOH capping agent were selected for the following experiments, due to smaller particle size and polydispersity.

The effect of zinc acetate concentration on the particle size and polydispersity was assessed for the Drop *In situ* method. As observed in Fig. 1.c) and d), there is a slight increase in ZnO particle size when zinc acetate increases up to 0.03 M (up to 244 nm). Increasing zinc acetate to 0.05 M, the particle size slightly decreased to 220 nm. When zinc acetate concentration is higher than 0.05 M, a significant (and uncontrolled) increase in particle size and polydispersity was observed. The effect of NaOH concentration was also tested. Results indicated an increase in particle size and polydispersity when higher concentrations of NaOH were used. Since the lowest concentration of NaOH (1 M) is already in excess in relation to $Zn(CH_3COO)_2$, the lowest concentration was chosen for further experiments. Considering these results, for the following experiments, a concentration of 0.05 M of $Zn(CH_3COO)_2$ and 1 M of NaOH were used for the synthesis of ZnO with BNC. Not only the particle size should be considered for the antimicrobial efficiency, but also the ZnO amount incorporated in the matrix (Gudkov et al., 2021). Therefore, the highest concentration was considered to maximise the BNC_{ZnO}

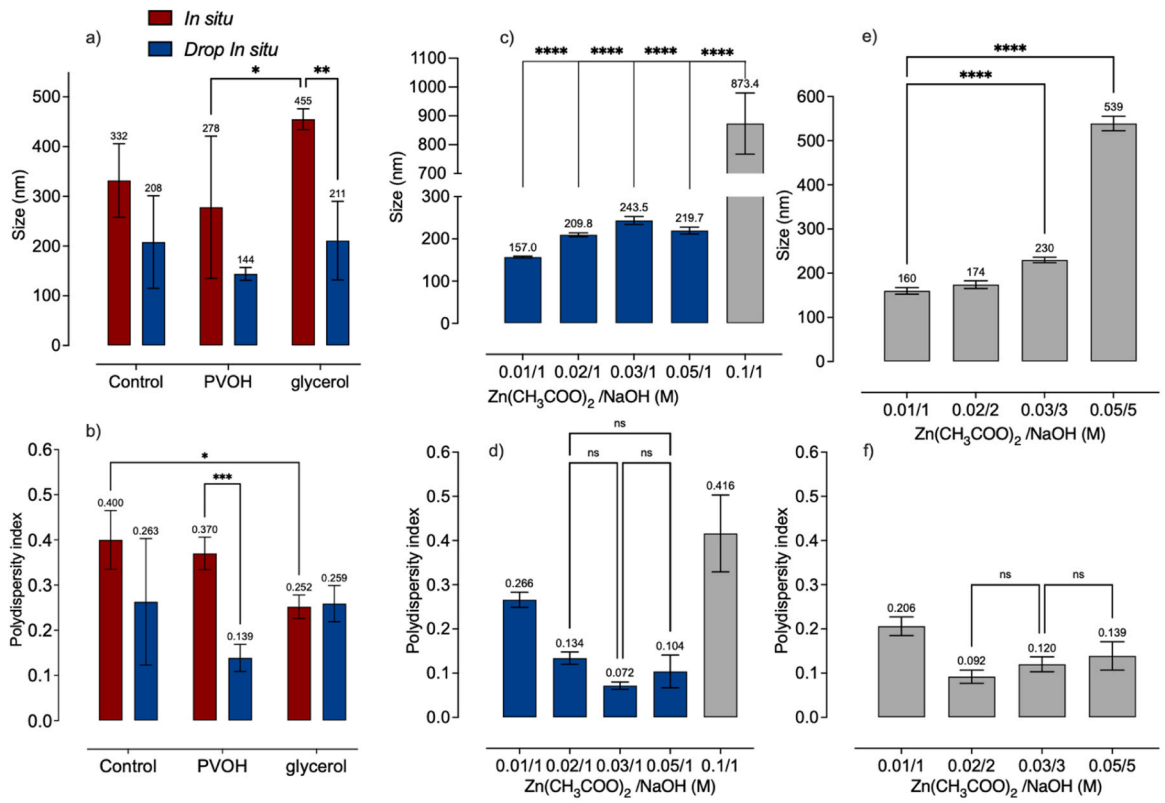

Fig. 1. ZnO particle size and polydispersity measurements by DLS: a,b) capping optimization with *In situ* and Drop *in situ* methods; c,d) $Zn(CH_3COO)_2$ concentration optimization for Drop *in situ* method; e,f) Sodium hydroxide concentration optimization for Drop *in situ* method; '* ' statistical different ($p < 0.05$); 'ns' stands for non-significant ($p > 0.05$);.

antimicrobial activity. Additionally, higher Zn migration is expected for films with higher Zn concentrations. Therefore, the migration is tested in more aggressive conditions.

3.2. ZnO particle size and Zn concentration in BNC_{ZnO} films

After BNC_{ZnO} production under optimized conditions, ZnO particles were characterized regarding their distribution throughout the fibre network of BNC, particle size (measured from SEM-EDS images) and the amount of ZnO on the BNC_{ZnO}. The distribution of ZnO on the BNC_{ZnO} 3D network was observed by SEM in the middle and the edge of the cross-section. Fig. 2a shows images of the fibre network of neat BNC and with impregnated NPs (identified by EDS). Concerning BNC_{ZnO}, ZnO particles were found to be well distributed either in the middle and the edge areas, meaning that the dropwise addition of NaOH led to a well distributed formation of ZnO NPs throughout the 3D matrix. Ensuring a well distribution of the ZnO particles is of great importance since it may affect the antimicrobial efficiency of the functionalised material.

Regarding the particle size distribution (see Fig. 2b), using Zn $(CH_3COO)_2$ at a concentration of 0.05 M led to particle agglomeration, with particles sizes as high as 1150 nm. The most frequent particle size found was 250 nm (with relative frequency of 20%). Additionally, high polydispersity of ZnO particles was found on the BNC matrix (150–1050 nm of ZnO). These results showed that BNC may have affected the ZnO synthesis, since higher particles sizes and polydispersity were observed when compared to DLS data (Fig. 1.c) and d) *vs* Fig. 2b). Still, the use of 0.05 M $Zn(CH_3COO)_2$ allowed a significant ZnO synthesis in the BNC (270 $mg.L^{-1}$ of Zn was found on BNC_{ZnO} quantified by AAS; BNC_{ZnO} (mg): 6.50 ± 1.10; ZnO (mg): 2.84 ± 0.37).

3.3. FTIR spectra

Fig. 3 displays the FTIR spectra of BNC, BNC_{ZnO} and ZnO. BNC and BNC_{ZnO} exhibited similar vibration bands, namely at 1000–1200 and 1300–1400 cm^{-1}, assigned to C-O bonds and C-H bending, respectively. BNC and BNC_{ZnO} also displayed bands around 3300–3400 cm^{-1}, related to the O-H groups of water (Mota et al., 2022). The BNC_{ZnO} spectra features a peak at 350–400 cm^{-1}, which regards Zn-O bond oscillation (Gharoy Ahangar et al., 2015). The ZnO spectra were also obtained, where it may be observed the same Zn-O peak 400–350 cm^{-1}.

3.4. Migration tests

3.4.1. Migration into ethanolic solutions

The BNC_{ZnO} produced by the Drop *in situ* method was submitted to migration studies, carried out using ethanol solutions as food simulants, at 10%, 20% and 50% (v/v). The simulants with 10% and 50% (v/v) ethanol, according to Regulation (EU) No. 10/2011, must be used for materials intended to be in contact with meat-based products. An intermediate concentration of ethanol was additionally included in the study, which is also foreseen in the regulation for processed fish, fruits and vegetables among other products. Migration tests with simulants were conducted at 60 °C for 15 days and the released Zn was quantified. The concentration values in the liquid simulants were converted into mg per kg of food using the solutions density. The observed Zn migration kinetics is presented in Fig. 4.a).

Higher values of Zn migration into simulants with lower ethanol concentrations were found. This could be expected since Zn has higher solubility in water than in ethanol, as elsewhere reported (Huang et al., 2017). Similar results were reported for Zn migration from low density polyethylene-ZnO (LDPE-ZnO) films tested against different simulants (ethanol 10%, acetic acid 4%, distilled water and n-heptane). In those

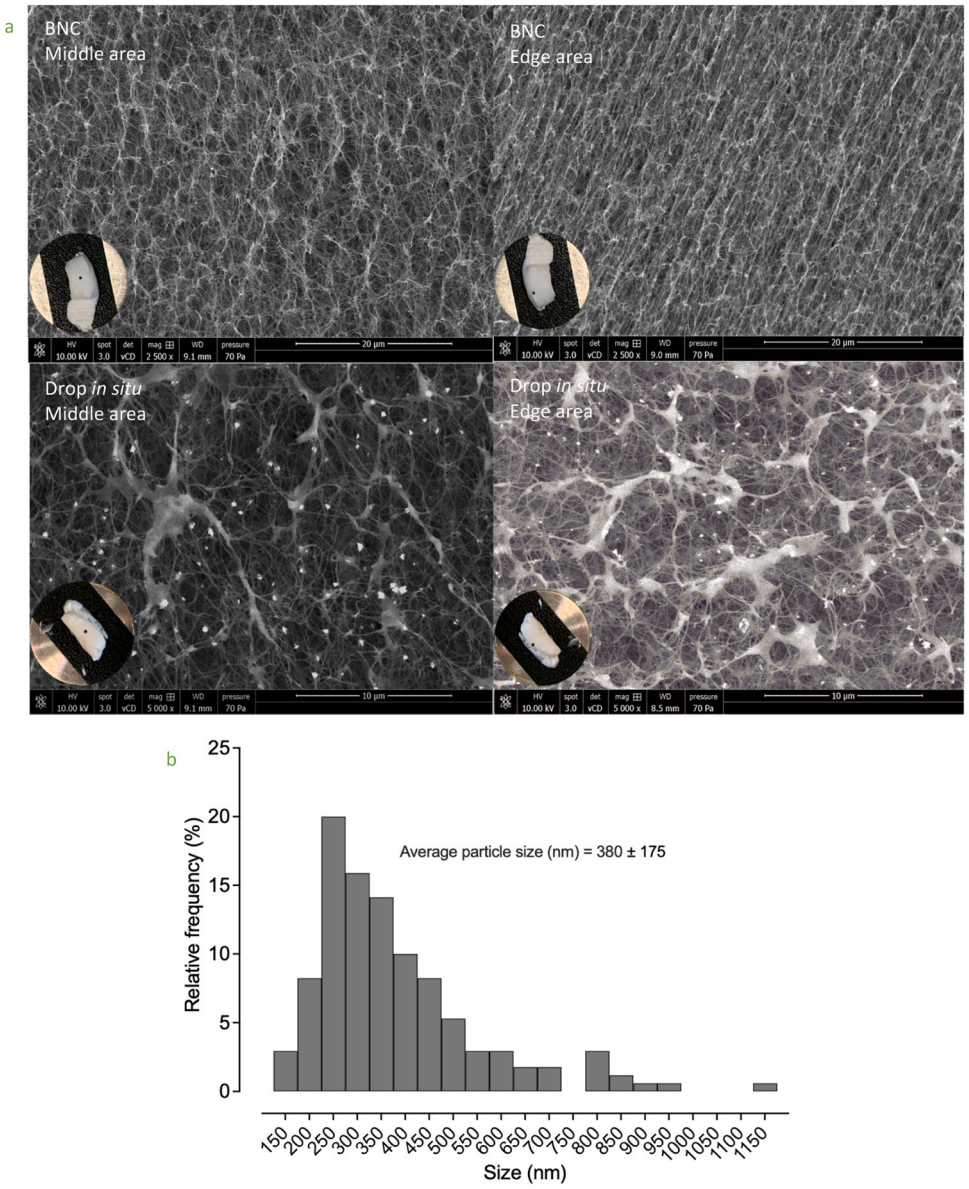

Fig. 2. SEM images of the cross section of neat BNC and BNC_{ZnO} disks; ZnO particle size distribution (measured from SEM images), Zn concentration and estimated mass of ZnO (mg) incorporated in BNC_{ZnO} using 0.05 M of $Zn(CH_3COO)_2$.

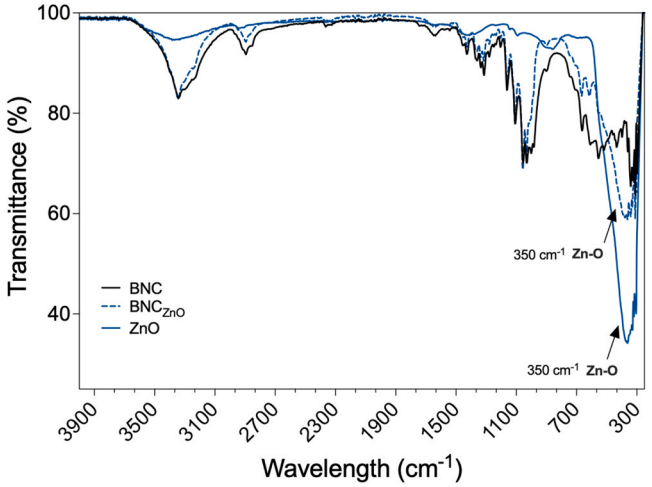

Fig. 3. FTIR spectrum of BNC, BNC_{ZnO} and ZnO nanoparticles.

studies, Zn migration was directly correlated with Zn solubility on each food simulant (Polat et al., 2018).

Concerning the migration kinetics (Fig. 4.a)), for the lower ethanol concentrations an increase in zinc migration was observed in the initial 8 h, whereas for EtOH50% migration occurred within 2 h; then, an equilibrium seems to have been reached in the next 72 h, no significant differences in concentration being observed ($p > 0.05$). However, after 72 h of contact, a continuous decrease of Zn in the liquid phase took place in all simulants, down to 0.44 mg L^{-1} after 15 days, suggesting that there was a reabsorption of Zn by the BNC_{ZnO} ($p < 0.05$). This is a surprising result, but reabsorption of migrants from cellulose-based materials has previously been reported in the literature (Poças et al., 2011).

Zn was detected in all food simulants at levels between 0.39 and 3.6 mg L^{-1} (Fig. 4.a)), which corresponds to a level of extraction from the BNC between 0.1% and 0.7%, considering that BNC_{ZnO} contains an average of ZnO of 270 mg L^{-1} (Table S3). The migration levels obtained with BNC_{ZnO} in these food simulants were below the specific migration limit (SML) for soluble ionic zinc (5 mg kg^{-1} food) set out by the

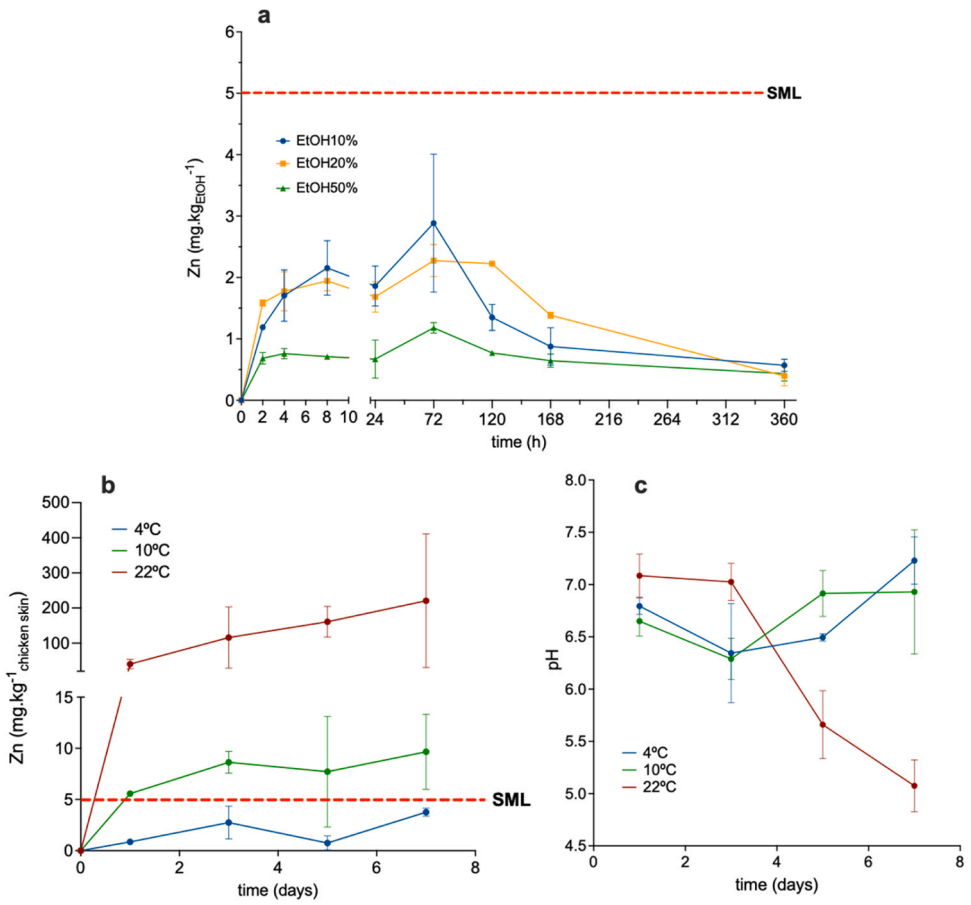

Fig. 4. Fig. 4. Zn migration from BNC_{ZnO}. a) Migration into food simulants (EtOH 10%, 20% and 50%) at 60 °C; b) Migration into chicken at 4, 10 and 22 °C; c) pH of the chicken skin during migration tests.

European Plastics Regulation (EU) 2016/1416 amending and correcting Regulation (EU) 10/2011 (European Parliament and Council, 2018).

It is important to mention that only Zn migration was quantified in this assay, and no distinction was made between migration of ZnO NPs or Zn in its ionic form. As previously mentioned, EFSA concluded that ZnO NPS does not migrate in its nanoform, if incorporated in an unplasticized polymer (Commission, 2007; EFSA CEF Panel, 2017). However, the possible migration of ZnO in nanoform from cellulosic materials should not be ruled out. The migration of ZnO NPs may occur through diffusion and its extent of migration may depend on the particle shape and size of ZnO as well as on the properties of the BNC (such porosity and surface area) (Kim et al.,2022; Zhao et al., 2018). Several reasons lead us to consider that most of Zn migration occurs in its ionic form (Zn^{2+}). As perceived in Fig. 2. b, high particles sizes were produced inside the BNC, which may hinder ZnO migration in its nanoform (low migration rates observed in Fig. 4.a)). Also, nanocellulose (including BNC) can act as adsorbent (of ZnO or Zn^{+2}) due to high surface area, full of surface hydroxyl groups, which facilitates the interaction with ZnO *via* hydrogen bonding (Hu et al., 2010; Sayyed et al., 2021; Zou et al., 2019). This adsorption ability is also seen after 120 h of Zn migration (Fig. 4. a)). Despite BNC having a highly porous structure, which eased the incorporation of $Zn(CH_3COO)_2$ and NaOH for ZnO synthesis, this porous structure was subsequently reduced after BNC_{ZnO} drying process, hindering as well the ZnO migration in its nanoform. As described in the experimental section, BNC_{ZnO} was air dried. Upon drying, water molecules that maintain the fibre separation are lost, leading to hornification, a process that permanently agglomerates and stacks the cellulose fibres (Martins et al., 2020).

3.4.2. *Migration into chicken skin*

Following the migration tests with ethanol aqueous solutions, a more realistic model was taken to assess the Zn migration from the BNC_{ZnO}. The values of Zn migration into chicken skin are depicted in Fig. 4.b). The temperature showed to play a very relevant effect on the amount of migrated Zn through time. Most of the release is observed on the first day, slight increasing in the following days. Migration increases with the temperature, specially between 10 and 22 °C. In contrast to the results obtained with ethanol simulants (Fig. 4. a)), Zn migration to chicken skin was much higher, in particular at higher temperatures. Only at 4 °C, the Zn migration was below the SML (5 mg kg^{-1} food), in agreement with the results obtained using simulants. The Zn level of extraction after 7 days of contact was 0.20% at 4 °C, 0.62% at 10 °C and 14.12% at 22 °C (Table S4).

At early stages (until day 3), Zn migration occurs due to the difference in concentration (not in equilibrium) and the migration rate increases with temperature. However, at a later stage (after 3 days) of the migration process, a slight Zn release was observed in the assay at 22 °C, which is explained by the acidification of chicken skin over time (Fig. 4. b). As reported elsewhere, the release of Zn^{2+} was much higher at an acidic pH than at neutral one (Hakeem et al., 2020). Indeed, ZnO is much more soluble in acidic solutions, such as 4% v/v acetic acid (Bumbudsanpharoke et al., 2019), explaining the higher migration to chicken skin at 22 °C (Fig. 4.b). At lower temperatures (4 °C and 10 °C), pH values were maintained throughout the assay, therefore, the migration occurred to a much lower extent (Fig. 4.c).

There is plenty of published literature addressing the role of ZnO as antimicrobial and the Zn migration into food simulants, but studies focusing on migration into meat products are scarce. Some of the data available concern the migration to raw chicken (Hakeem et al., 2020)

and pork (Xiao et al., 2020). The Zn migration from functionalized absorbing pad into raw chicken meat was determined with levels that did not surpass 5.0 mg kg^{-1}, after 8 days at 4 °C (Hakeem et al., 2020). The Zn migration from a nanocomposite film of soy protein isolate reinforced with cellulose nanocrystals and ZnO NP gave Zn migration into pork up to 20.0 mg kg^{-1} after 6 days at 4 °C on pork (Xiao et al., 2020). However, those studies do not indicate the pH values of the meat, which is a key parameter, as it is shown in this work. Acidification does have an additional impact on Zn migration rate.

3.4.3. Simulation of Zn migration using the Weibull model

The Weibull kinetic model was fitted to the experimental data obtained for the Zn migration from BNC onto chicken skin. The model parameters were estimated for each temperature (Table S5). The relevance of C∞ , τ and β in the model (model fitting) was assessed statistically, by using the 95% confidence interval (parameter is different from 0). The model showed good fitting for 4 °C, with estimated C∞ and τ (statistically different from 0). On the other hand, β was not statistically different from zero, which indicated that this parameter is not relevant in the model. At higher temperatures, the model parameters showed higher error estimations, specially at 22 °C (Table S5). At this high temperature, the model does not describe well the experimental data, and a clear distinctive migration pattern occurs throughout the assay, due to the change of the skin's pH, that highly increases the Zn migration (Figs. 4.c and 5).

The shape of the Zn migration curves is well represented by the Weibull model only for Zn migration at 4 °C and 10 °C. The effect of temperature in the model parameters is also represented in Fig. 5. An exponential effect of temperature in the equilibrium concentration (C∞) is observed (R^2 =0.9995), possibly due to the direct effect of temperature combined with the indirect effect on pH, both affecting the zinc solubility and therefore the equilibrium concentration on the food model. Solubility parameters were used in several migration studies to predict migrant's behaviour onto food (Gavriil et al., 2018).

The effect of temperature on the rate of the process (τ parameter) follows an Arrhenius-like pattern (R^2 = 0.9624), and the values of τ ranged from 0.5 to 2.8. Similar observation can be made to β, the behavioural index relating to the initial rate of the process, increased with temperature, following the Arrhenius behaviour (R^2 = 0.903). However, due to the different behaviour of the system observed at 22 °C, the relationship shown in Fig. 5 is merely indicative as only two valid temperatures (the lower ones) can be considered. It is recognised that to develop a model to simulate the migration of zinc from BNC_{ZnO} on chicken skin and to consider the effect of temperature on the model parameters, data with more temperature levels are required, specially within the range of interest related to the conditions of storage and retailing of the products represented by this food model.

As observed in Figs. 4.b) and 5, Zn migration surpassed the SML (5.0 mg kg^{-1}) at temperatures higher than 10 °C. Although prescribed storage temperatures for meat products are in the range of 4 °C, temperature fluctuations may occur along the food chain supply, triggering higher Zn migration rates. This is a limitation of the developed BNC_{ZnO} films, where Zn migration can surpass the SML for higher storage temperatures. To counteract this, strategies should be established to delay Zn migration. Modification of the BNC_{ZnO} surface by coating with poly (3-hydroxybutyrate-co-3-hydroxyvalerate) (PHBV), for example, may delay Zn migration. While other authors have reported the difficulty of incorporating ZnO in polymers such PHBV (low adhesion), this may actually favour lower migration rates (Râpă et al., 2021), as the ability of coating BNC with PHBV has been demonstrated in previous work (Soares da Silva et al., 2022). However, a coating may compromise the antibacterial efficiency. Therefore, more research should be done, considering the type of coating used and the grammage applied on the composite, in order to optimize both antibacterial activity and Zn migration.

3.5. BNC_{ZnO} antimicrobial performance on chicken

The films based on BNC_{ZnO} may find an interesting application as an antimicrobial packaging material for meat-based products such as chicken. Therefore, antimicrobial studies with BNC_{ZnO} were carried out on chicken skin contaminated with *Salmonella (S. Enteritidis* and cocktail*), E. coli* and *Campylobacter (C. coli* and cocktail*),* common bacteria found in chicken. Only Gram-negative bacteria were assessed because previous work has shown that ZnO was mainly effective against these bacteria. Untreated chicken skin samples (without BNC/BNC_{ZnO}) were

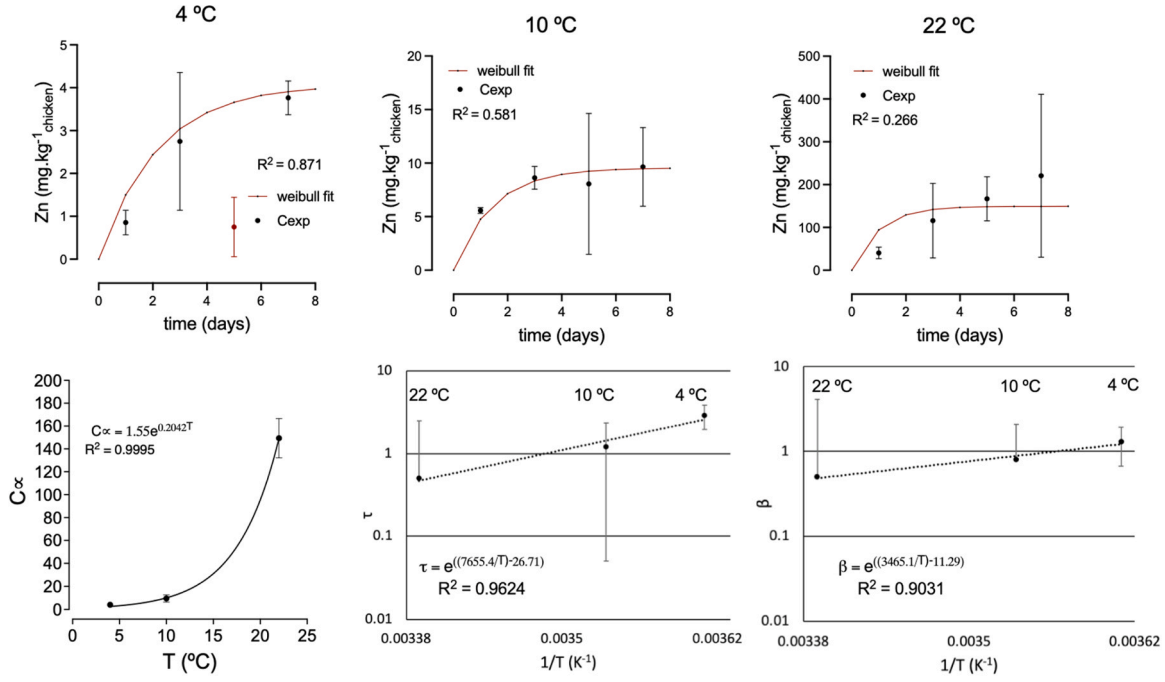

Fig. 5. Zn migration from BNC onto chicken skin at 4 °C, 10 °C and 22 °C, and Weibull parameters estimated for each temperature (Data point at 4 °C, 5 days of contact, coloured in red, not used for modelling).

also tested as a control.

Fig. 6 shows the results of cell counts over time. Overall, in the first 24 h (up to the point where disks were applied), the number of active growing cells remained constant, for all the bacteria tested. After application of the BNC_{ZnO} disks, the number of active growing cells was reduced while counts in chicken samples without any disk remained constant. For *E. coli* and *Salmonella (S.* Enteritidis and cocktail), a 0.5 log reduction was obtained after 24 h hour contact. For *Campylobacter* strains, higher inhibition was observed when BNC_{ZnO} was in contact with the contaminated chicken skin samples (2.0–2.5 log reduction after 24 h). A slight reduction was also observed for the BNC film without ZnO for the *Campylobacter* cocktail. These results indicate that the BNC_{ZnO} films have antimicrobial effect (especially against *Campylobacter* species) on chicken, in agreement with other works that showed antimicrobial effect of ZnO NPs against pathogens on chicken meat samples (Amjadi et al., 2019; Hakeem et al., 2020; Pirsa et al., 2018).

However, the antimicrobial effect against *E. coli* and *Salmonella* may be considered too low, if considering the Zn migration level on chicken skin at 4 °C, where SML was almost reached (Figs. 4 and 5). Thus, the developed composite still has room for improvement, to increase the antimicrobial effect without increasing the Zn migration levels. This study shows the importance of performing both antimicrobial and migration tests as both mechanisms are important and often correlated when developing an active packaging.

4. Conclusions

Active food packaging has become a very attractive research field. Among the active substances, zinc oxide nanoparticles (ZnO) have been explored due to their antimicrobial properties, whereas bacterial nanocellulose (BNC) has been explored as a carrier for active agents. In this study a BNC_{ZnO} film was successfully developed, using Drop *in situ* method, which relied on the dropwise addition of NaOH (1 M) to BNC pellicles immersed in zinc acetate solution. Through this method, the ZnO was homogenously distributed within the BNC network (confirmed by SEM-EDS), in the form of nanoparticles with sizes ranging 100–300 nm. The increase of $Zn(CH_3COO)_2$ concentration as precursor of ZnO particles promotes the increase of the amount of ZnO retained in the BNC matrix, but also leads to larger particle size, with lower specific surface area which can compromise the antimicrobial activity.

The migration tests using food simulants revealed low migration values (lower than SML), with some reabsorption effect after 8 h of contact. In the test of Zn migration into a real food model as chicken skin no reabsorption effect occurred, and Zn migration was temperature and pH dependent. The migration values at 4 °C were lower than the SML, while at higher temperatures (10 °C and 22 °C) SML was surpassed. The Weibull model was fit to the migration experimental data and the parameters concentrations at equilibrium (C_∞), Zn migration rate (τ) and behavioural index relating to the initial rate of the process (β) were estimated at the tested temperatures. The model allows predicting the migration of Zn under different conditions when BNC_{ZnO} is in contact with chicken skin, important information before considering the feasibility of using these materials in active food packaging. The antibacterial activity of BNC_{ZnO} films was also observed, against *Salmonella* spp., *E. coli* and *Campylobacter* spp., using chicken skin as a food model. In sum, BNC_{ZnO} shows a potential for use as an antimicrobial packaging film for fresh/conditioned chicken.

Funding

This article/publication is based upon work co-financed by Fundo Europeu de Desenvolvimento Regional (FEDER), through the Programa Operacional Competitividade e Internacionalização (POCI), under the scope of the project BIOPROTECT Development of Biodegradable Packaging Material with Active Properties for Food Preservation - POCI-01-0247-FEDER-069858. This study was also supported by FCT under the scope of the strategic funding of UIDB/50016/2020 and UID/BIO/04469 units and by LABBELS – Associate Laboratory in Biotechnology, Bioengineering and Microelectromechanical Systems, LA/P/0029/2020. The authors also acknowledge the financial support of the FCT (ESF) through the grant given to Francisco A.G. Soares Silva (SFRH/BD/146375/2019).

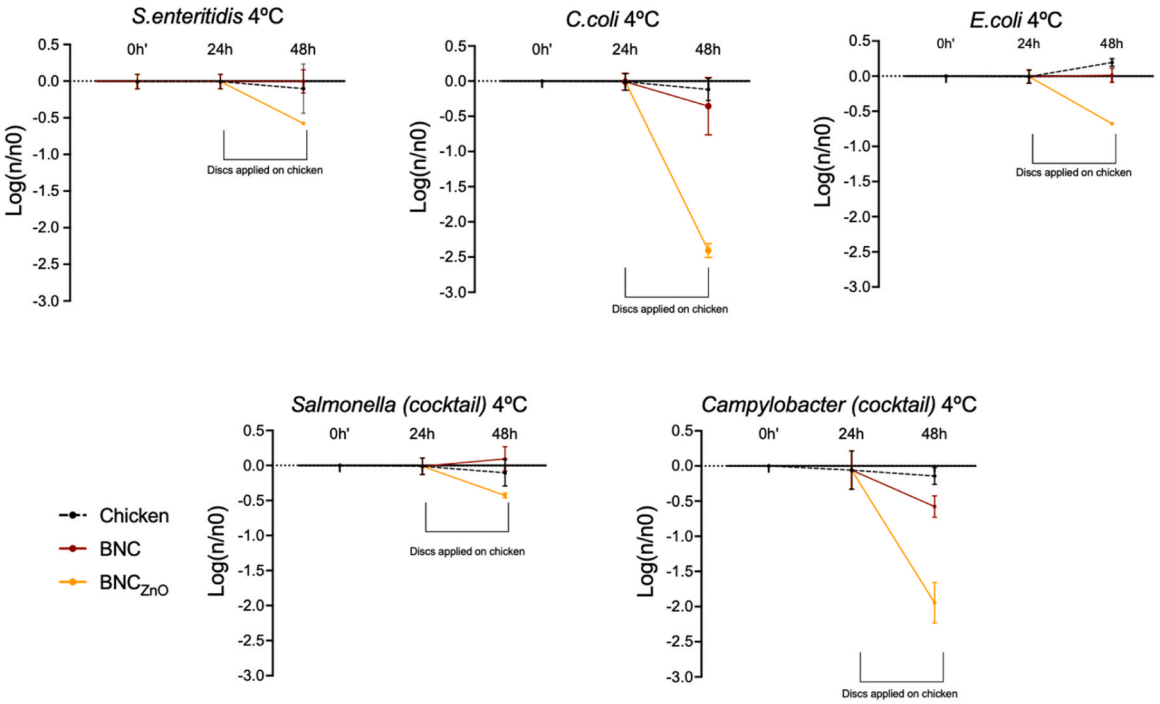

Fig. 6. Viable cell count for *E. coli, Salmonella* and *Campylobacter* on skin chicken, when exposed to BNC_{ZnO} and controls (BNC and chicken inoculated without any disk).

CRediT authorship contribution statement

Francisco A.G. Soares Silva: Investigation, Methodology, Formal analysis, Writing – original draft, Writing – review & editing. **Teresa Bento de Carvalho**: Investigation, Methodology. **Fernando Dourado:** Conceptualization, Writing – review & editing. **Miguel Gama:** Conceptualization, Writing – review & editing. **Paula Teixeira:** Conceptualization, Writing – review & editing, **Fátima Poças:** Supervision, Conceptualization, Writing – review & editing.

Declaration of Competing Interest

The authors declare that they have no known competing financial interests or personal relationships that could have appeared to influence the work reported in this paper.

Data Availability

Data will be made available on request.

Acknowledgements

The authors appreciate the technical support from CINATE team, especially Susana Teixeira for the assistance in atomic absorption spectroscopy.

Appendix A. Supporting information

Supplementary data associated with this article can be found in the online version at doi:10.1016/j.fpsl.2023.101140.

References

Almasi, H., Mehryar, L., & Ghadertaj, A. (2019). Characterization of CuO-bacterial cellulose nanohybrids fabricated by in-situ and ex-situ impregnation methods. *Carbohydrate Polymers, 222*, Article 114995.

Amjadi, S., Emaminia, S., Nazari, M., Davudian, S. H., Roufegarinejad, L., & Hamishehkar, H. (2019). Application of reinforced ZnO nanoparticle-incorporated gelatin bionanocomposite film with chitosan nanofiber for packaging of chicken fillet and cheese as food models. *Food and Bioprocess Technology, 12*(7), 1205–1219. https://doi.org/10.1007/s11947-019-02286-y

Bumbudsanpharoke, N., Choi, J., Jin, H., & Ko, S. (2019). Zinc migration and its effect on the functionality of a low density Polyethylene-ZnO nanocomposite film. *Food Packging Shelf Life, 20*(January). https://doi.org/10.1016/j.fpsl.2019.100301

Cazón, P., & Vázquez, M. (2021). Bacterial cellulose as a biodegradable food packaging material: a review. *Food Hydrocolloids, 113*, Article 106530.

Cerqueira, M. A., Torres-Giner, S., & Lagaron, J. M. (2018). *Nanostructured multilayer films. Nanomaterials for food packaging: Materials, processing technologies, and safety issues*. Elsevier Inc. https://doi.org/10.1016/B978-0-323-51271-8.00006-1

Choo, K. W., Dhital, R., Mao, L., Lin, M., & Mustapha, A. (2021). Development of polyvinyl alcohol/chitosan/modified bacterial nanocellulose films incorporated with 4-hexylresorcinol for food packaging applications. *Food Packaging and Shelf Life, 30*, Article 100769.

Commission, T. H. E. E. (2007). Opinion of the Scientific Panel on food additives, flavourings, processing aids and materials in contact with food (AFC) related to a 16th list of substances for food contact materials. *EFSA Journal, 5*(10), 22–42. https://doi.org/10.2903/j.efsa.2007.555

de Amorim, J. D. P., de Souza, K. C., Duarte, C. R., et al. (2020). Plant and bacterial nanocellulose: Production, properties and applications in medicine, food, cosmetics, electronics and engineering. A review. *Environmentl Chemistry Letter, 18*, 851–869. https://doi.org/10.1007/s10311-020-00989-9

Dileswar, Pradhan, Jaiswal, Amit K., & Jaiswal, Swarna (2022). Nanocellulose based green nanocomposites: characteristics and application in primary food packaging. *Food Reviews International*. https://doi.org/10.1080/87559129.2022.2143797

EFSA CEF Panel. (2017). Safety assessment of the substance zinc oxide, nanoparticles, for use in food contact materials. *EFSA Journal* (Vol. 14). https://doi.org/10.2903/j.efsa.2016.4408

European Parliament and Council. (2018). *Directive (EU) 2018/852 of the European Parliament and of the Council of 30 May 2018 amending Directive 94/62/EC on packaging and packaging waste. Official Journal of th*e European Union, 2018 (November 2008), 141–154. Retrieved from ⟨https://eur-lex.europa.eu/legal-content/EN/TXT/PDF/?uri=CELEX:32018L0852⟩.

European Standard (2013). *Foodstuffs-determination of elements and their chemical species-general considerations and specific requirements* (EN 13804: 2013).

Jedrzejczak-Krzepkowska, M., Kubiak, K., Ludwicka, K., & Bielecki, S. (2016). - Bacterial nanocellulose synthesis, recent findings. In M. Gama, F. Dourado, & S. Bielecki (Eds.), *Bacterial nanocellulose*. Amsterdam: Elsevier.

Gavriil, G., Kanavouras, A., & Coutelieris, F. A. (2018). Food-packaging migration models: A critical discussion. *Critical Reviews in Food Science and Nutrition, 58*(13), 2262–2272. https://doi.org/10.1080/10408398.2017.1317630

Gharoy Ahangar, E., Abbaspour-Fard, M. H., Shahtahmassebi, N., Khojastehpour, M., & Maddahi, P. (2015). Preparation and Characterization of PVA/ZnO Nanocomposite. *Journal of Food Processing and Preservation, 39*(6), 1442–1451. https://doi.org/10.1111/jfpp.12363

Gudkov, S. V., Burmistrov, D. E., Serov, D. A., Rebezov, M. B., Semenova, A. A., & Lisitsyn, A. B. (2021). A mini review of antibacterial properties of ZnO nanoparticles. *Frontiers in Physics, 9*, Article 641481.

Hakeem, M. J., Feng, J., Nilqhaz, A., Seah, H. C., Konkel, M. E., & Lua, X. (2020). Active packaging of immobilized zinc oxide nanoparticles controls campylobacter jejuni in raw chicken meat. *Applied and Environmental Microbiology, 86*(22). https://doi.org/10.1128/AEM.01195-20

Hallinan, A. J. (1993). A review of the weibull distribution. *Journal of Quality Technology, 25*(2), 85–93. https://doi.org/10.1080/00224065.1993.11979431

Hestrin, S., & Schramm, M. (1954). Synthesis of cellulose by Acetobacter xylinum. II. Preparation of freeze-dried cells capable of polymerizing glucose to cellulose. *The Biochemical Journal, 58*(2), 345–352. https://doi.org/10.1042/bj0580345

Hu, W., Chen, S., Zhou, B., & Wang, H. (2010). Facile synthesis of ZnO nanoparticles based on bacterial cellulose. *Materials Science and Engineering: B, 170*(1–3), 88–92.

Huang, H., Tang, K., Luo, Z., Zhang, H., & Qin, Y. (2017). Migration of Ti and Zn from nanoparticle modified ldpe films into food simulants. *Food Science and Technology Research, 23*(6), 827–834.

Ibrahim, N. I., Shahar, F. S., Sultan, M. T. H., Shah, A. U. M., Safri, S. N. A., & Mat Yazik, M. H. (2021). Overview of bioplastic introduction and its applications in product packaging. *Coatings, 11*(11), 1423.

Kim, I., Viswanathan, K., Kasi, G., Thanakkasaranee, S., Sadeghi, K., & Seo, J. (2022). ZnO nanostructures in active antibacterial food packaging: Preparation methods, antimicrobial mechanisms, safety issues, future prospects, and challenges. *Food Reviews International, 38*(4), 537–565.

Kishore, A., Aravind, S. M., & Singh, A. (2023). Bionanocomposites for active and smart food packaging: A review on its application, safety, and health aspects. *Journal of Food Process Engineering, 46*(5), Article e14320. https://doi.org/10.1111/jfpe.14320

Kumar, R., Umar, A., Kumar, G., & Nalwa, H. S. (2017). Antimicrobial properties of ZnO nanomaterials: A review. *Ceramics International, 43*(5), 3940–3961. https://doi.org/10.1016/j.ceramint.2016.12.062

Martins, D., de Carvalho Ferreira, D., Gama, M., & Dourado, F. (2020). Dry Bacterial Cellulose and Carboxymethyl Cellulose formulations with interfacial-active performance: processing conditions and redispersion. *Cellulose, 27*, 6505–6520.

Missio, A. L., Mattos, B. D., Ferreira, D., de, F., Magalhães, W. L. E., Bertuol, D. A., Gatto, D. A., Pettschnigg, A., & Tondi, G. (2018). Nanocellulose-tannin films: From trees to sustainable active packaging. *Journal of Cleaner Production, 184*, 143–151. https://doi.org/10.1016/j.jclepro.2018.02.205

Mota, R., Rodrigues, A. C., Silva-carvalho, R., Costa, L., Martins, D., Sampaio, P., Dourado, F., & Gama, M. (2022). Tracking bacterial nanocellulose in animal tissues by fluorescence. *Microscopy*, 1–20.

Olaimat, A. N., Sawalha, A. G. A., Al-Nabulsi, A. A., Osaili, T., Al-Biss, B. A., Ayyash, M., & Holley, R. A. (2022). Chitosan–ZnO nanocomposite coating for inhibition of Listeria monocytogenes on the surface and within white brined cheese. *Journal of Food Science, 87*(7), 3151–3162. https://doi.org/10.1111/1750-3841.16208

Pan, X., Li, J., Ma, N., Ma, X., & Gao, M. (2023). Bacterial cellulose hydrogel for sensors. *Chemical Engineering Journal, 461*, Article 142062.

Pirsa, S., Shamusi, T., & Kia, E. M. (2018). Smart films based on bacterial cellulose nanofibers modified by conductive polypyrrole and zinc oxide nanoparticles. *Journal of Applied Polymer Science, 135*(34), 1–10. https://doi.org/10.1002/app.46617

Poças, F., Franz, R. (2018). *Overview on european regulatory issues, legislation, and EFSA evaluations of nanomaterials. In Nanomaterials for Food Packaging: Materials, Processing Technologies, and Safety Issues* (pp. 277–300). https://doi.org/10.1016/B978–0-323–51271-8.00010–3.

Poças, M., de, F., Oliveira, J. C., Pereira, J. R., Brandsch, R., & Hogg, T. (2011). Modelling migration from paper into a food simulant. *Food Control, 22*(2), 303–312. https://doi.org/10.1016/j.foodcont.2010.07.028

Poças, M. F., Oliveira, J. C., Brandsch, R., & Hogg, T. (2012). Analysis of mathematical models to describe the migration of additives from packaging plastics to foods. *Journal of Food Process Engineering, 35*(4), 657–676. https://doi.org/10.1111/j.1745-4530.2010.00612.x

Polat, S., Fenercioğlu, H., & Güçlü, M. (2018). Effects of metal nanoparticles on the physical and migration properties of low density polyethylene films. *Journal of Food Engineering, 229*, 32–42. https://doi.org/10.1016/j.jfoodeng.2017.12.004

Răpă, M., Stefan, M., Popa, P. A., Toloman, D., Leostean, C., Borodi, G., Vodnar, D. C., Wrona, M., Salafranca, J., Nerín, C., Barta, D. G., Suciu, M., Predescu, C., & Matei, E. (2021). Electrospun nanosystems based on PHBV and ZnO for ecological food packaging. *Polymers, 13*(13), 2123.

Sayyed, A. J., Pinjari, D. V., Sonawane, S. H., Bhanvase, B. A., Sheikh, J., & Sillanpää, M. (2021). Cellulose-based nanomaterials for water and wastewater treatments: A review. *Journal of Environmental Chemical Engineering, 9*(6), Article 106626.

Silva, F. A. G. S., Dourado, F., Gama, M., & Poças, F. (2020). Nanocellulose bio-based composites for food packaging. *Nanomaterials, 10*(10), 1–29. https://doi.org/10.3390/nano10102041

Sirelkhatim, A., Mahmud, S., Seeni, A., Kaus, N. H. M., Ann, L. C., Bakhori, S. K. M., Hasan, H., & Mohamad, D. (2015). Review on zinc oxide nanoparticles: Antibacterial

activity and toxicity mechanism. *Nano-Micro Letters, 7*(3), 219–242. https://doi.org/10.1007/s40820-015-0040-x

Soares da Silva, F. A. G., Matos, M., Dourado, F., Reis, M. A. M., Branco, P. C., Poças, F., & Gama, M. (2022). Development of a layered bacterial nanocellulose-PHBV composite for food packaging. *Journal of the Science of Food and Agriculture*. https://doi.org/10.1002/jsfa.11839

Gregor-Svetec, D. (2018). Intelligent packaging. *Nanomaterials for Food Packaging*, 203–247. https://doi.org/10.1016/B978-0-323-51271-8.00008-5

Tsai, Y. H., Yang, Y. N., Ho, Y. C., Tsai, M. L., & Mi, F. L. (2018). Drug release and antioxidant/antibacterial activities of silymarin-zein nanoparticle/bacterial cellulose nanofiber composite films. *Carbohydrate Polymers, 180*(August 2017), 286–296. https://doi.org/10.1016/j.carbpol.2017.09.100

Vilela, C., Kurek, M., Hayouka, Z., Röcker, B., Yildirim, S., Antunes, M. D. C., Nygaard, J. N., Pettersen, M. K., & Freire, C. S. R. (2018). A concise guide to active agents for active food packaging. *Trends in Food Science and Technology, 80*(August), 212–222. https://doi.org/10.1016/j.tifs.2018.08.006

Vilela, C., Moreirinha, C., Domingues, E. M., Figueiredo, F. M. L., Almeida, A., & Freire, C. S. R. (2019). Antimicrobial and conductive nanocellulose-based films for active and intelligent food packaging. *Nanomaterials, 9*(7), 1–16. https://doi.org/10.3390/nano9070980

Wahid, F., Duan, Y. X., Hu, X. H., Chu, L. Q., Jia, S. R., Cui, J. D., & Zhong, C. (2019). A facile construction of bacterial cellulose/ZnO nanocomposite films and their photocatalytic and antibacterial properties. *International Journal of Biological Macromolecules, 132*, 692–700. https://doi.org/10.1016/j.ijbiomac.2019.03.240

Wang, J., Tavakoli, J., & Tang, Y. (2019). Bacterial cellulose production, properties and applications with different culture methods–A review. *Carbohydrate polymers, 219*, 63–76.

Wojnarowicz, J., Chudoba, T., & Lojkowski, W. (2020). A review of microwave synthesis of zinc oxide nanomaterials: Reactants, process parameters and morphoslogies. *Nanomaterials, 10*(6). https://doi.org/10.3390/nano10061086

Xiao, Y., Liu, Y., Kang, S., Wang, K., & Xu, H. (2020). Development and evaluation of soy protein isolate-based antibacterial nanocomposite films containing cellulose nanocrystals and zinc oxide nanoparticles. *Food Hydrocolloids, 106*(April), Article 105898. https://doi.org/10.1016/j.foodhyd.2020.105898

Zhang, H., Yu, H. Y., Wang, C., & Yao, J. (2017). Effect of silver contents in cellulose nanocrystal/silver nanohybrids on PHBV crystallization and property improvements. *Carbohydrate Polymers, 173*, 7–16. https://doi.org/10.1016/j.carbpol.2017.05.064

Zhao, S. W., Guo, C. R., Hu, Y. Z., Guo, Y. R., & Pan, Q. J. (2018). The preparation and antibacterial activity of cellulose/ZnO composite: A review. *Open Chemistry, 16*(1), 9–20.

Zou, X. H., Zhao, S. W., Zhang, J. G., Sun, H. L., Pan, Q. J., & Guo, Y. R. (2019). Preparation of ternary ZnO/Ag/cellulose and its enhanced photocatalytic degradation property on phenol and benzene in VOCs. *Open Chemistry, 17*(1), 779–787.